mathematics

MDPI

Article

Application of Weighting Algorithm for Enhanced Broadband Vector Network Analyzer Measurements

Sang-hee Shin [1,*] and James Skinner [2]

[1] Department of Electrical Engineering, Sejong University, Seoul 05006, Republic of Korea
[2] National Physical Laboratory, Teddington TW11 0LW, UK; james.skinner@npl.co.uk
* Correspondence: ssh1625@sejong.ac.kr

Abstract: A weighting algorithm for application in the Thru-Reflect-Line (TRL) calibration technique is presented to enhance the accuracy and reliability of vector network analyzer (VNA) measurements over broad frequency bands. The method addresses the inherent limitations of the traditional TRL calibration, particularly the step changes observed in banded-TRL approaches when multiple Line standards are used. By introducing a bespoke weighting function that assigns phase-dependent weights to each Line standard, smoother transitions and improved S-parameter measurements can be achieved. Experimental validation using measurements of both 3.5 mm and Type-N devices demonstrates the effectiveness of the weighted-TRL method in eliminating discontinuities and calibration artifacts across a wide range of frequencies. The results reveal the improved calibration of S-parameters this approach can yield compared to traditional TRL calibration methods. The developed weighted-TRL calibration technique offers a significant advancement in metrology-grade measurements, enabling more precise characterization of high-frequency devices across broad frequency bands. By mitigating a key limitation of the TRL calibration, this method provides a valuable tool for enhancing the accuracy and reliability of VNA measurements for precision metrology applications.

Keywords: RF; microwave; S-parameters; VNA; 3.5 mm; Type-N

MSC: 68Q12

Citation: Shin, S.-h.; Skinner, J. Application of Weighting Algorithm for Enhanced Broadband Vector Network Analyzer Measurements. *Mathematics* **2024**, *12*, 2871. https://doi.org/10.3390/math12182871

Academic Editor: Fausto Sargeni

Received: 23 August 2024
Revised: 11 September 2024
Accepted: 13 September 2024
Published: 14 September 2024

1. Introduction

Accurate S-parameter measurements are essential for characterizing RF-microwave to millimeter-wave and terahertz (THz) devices and components in various fields, including telecommunications, wireless power transfer, quantum technologies, and semiconductor industries [1–3]. Vector network analyzers (VNAs) are the most essential instruments for such measurements, but their accuracy relies heavily on reliable error correction techniques [4–6]. Several two-port VNA calibration schemes have been developed by the VNA user community, the most commonly used being Short-Open-Load-Thru (SOLT) [7], Thru-Reflect-Match (TRM) [8], and Thru-Reflect-Line (TRL) [9].

This study focuses on the TRL calibration scheme, which is the scheme of choice for precision metrology. It is also particularly effective for applications such as cryogenic quantum technologies as it relies on the Line standards to supply the reference impedance. The lengths of a transmission line can be modelled very accurately, as compared with matched load standards used to provide the reference impedance in other calibration schemes such as SOLT and TRM [10]. Moreover, while schemes such as SOLT and TRM are widely used by the VNA user community, they require accurate knowledge of one or more of the calibration standards to be determined prior to the calibration. Therefore, these schemes are not suitable for primary-level calibration. As the TRL calibration has no such requirement, it is widely used for metrology-grade, primary-level calibration. This is evidenced by a recent interlaboratory comparison of measurements in high-frequency coaxial lines [11]

and other work on achieving broadband calibration accuracy from National Metrology Institutes (NMIs) [12–14].

However, the conventional TRL scheme suffers from its inherent frequency bandwidth limitations. The relative phase lengths of the Line standard determine the useful bandwidth of the calibration. By using multiple Line standards and joining the results, a banded-TRL can be employed to solve this problem. However, this banded-TRL method can introduce step changes or discontinuities in the calibrated S-parameter results at the transition frequencies between different Line standards [15].

This work introduces and compares weighted-TRL calibration methods employing bespoke weighting functions that assign frequency-dependent weights to each Line standard based on the relative phase change introduced by each. This approach facilitates seamless transitions between the calibration results pertaining to each Line standard, eliminating discontinuities in a metrologically coherent manner. Experimental validation using measurements of both 3.5 mm and Type-N coaxial devices is presented to demonstrate the method's efficacy in removing calibration failures and discontinuities. These methods are especially valuable in scenarios with limited Line standard availability, as well as in applications requiring non-standard custom calibration standards and algorithms, such as for microwave metrology in cryogenic environments [16,17].

2. VNA Calibration

2.1. The TRL Calibration Algorithm

Before conducting S-parameter measurements, it is crucial to perform accurate VNA calibrations. As shown in Figure 1a, the calibration process is performed to determine error parameters (error boxes A and B) for each port. By de-embedding the error boxes, unwanted effects, including error terms such as source match, directivity, and reflection tracking, are removed from the measurements, hence moving the measurement reference planes to the ports of the device under test (DUT), as shown in Figure 1a.

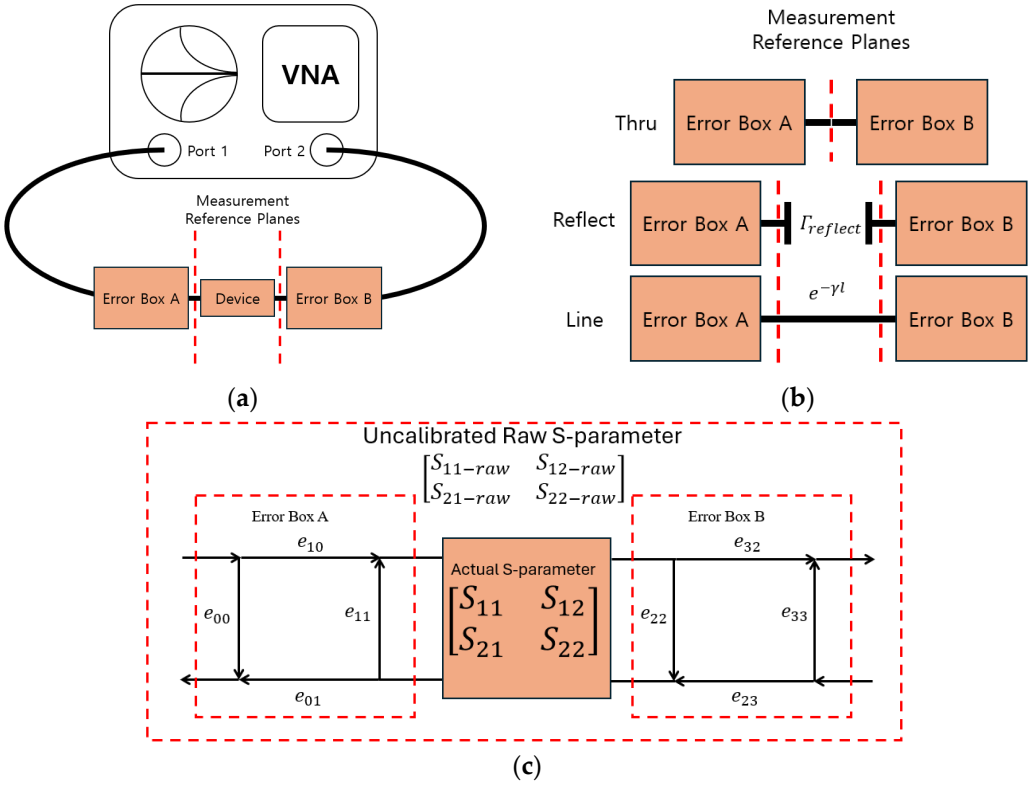

Figure 1. (**a**) VNA calibration; (**b**) TRL calibration standards; (**c**) TRL error matrix.

The TRL calibration scheme, which is the baseline calibration scheme in this work, only requires measurements of three calibration standards at minimum: a zero-length 'thru', a high reflect (providing equivalent reflection at each port), and a Line standard, as shown in Figure 1b. These measurements are applied to an eight-term error model, as shown in Figure 1c. Error parameters from error box A and B can be converted to cascade error matrices as follows:

$$E_A = \begin{bmatrix} \frac{(-e_{00}e_{11}+e_{10}e_{01})}{e_{10}} & \frac{e_{00}}{e_{10}} \\ -\frac{e_{11}}{e_{10}} & \frac{1}{e_{10}} \end{bmatrix}, \; E_B = \begin{bmatrix} \frac{(-e_{22}e_{33}+e_{32}e_{23})}{e_{32}} & \frac{e_{22}}{e_{32}} \\ -\frac{e_{33}}{e_{32}} & \frac{1}{e_{32}} \end{bmatrix}$$

Uncalibrated ($S_{11-raw}, S_{21-raw}, S_{12-raw}, S_{22-raw}$) and ideal ($S_{11}, S_{21}, S_{12}, S_{22}$) S-parameters of the calibration standards can be converted to cascade matrices as follows:

$$R_{meas} = \begin{bmatrix} \frac{(-S_{11-raw}S_{22-raw}+S_{12-raw}S_{21-raw})}{S_{21-raw}} & \frac{S_{11-raw}}{S_{21-raw}} \\ -\frac{S_{22-raw}}{S_{21-raw}} & \frac{1}{S_{21-raw}} \end{bmatrix}, \; R_{ideal} = \begin{bmatrix} \frac{(-S_{11}S_{22}+S_{12}S_{21})}{S_{21}} & \frac{S_{11}}{S_{21}} \\ -\frac{S_{22}}{S_{21}} & \frac{1}{S_{21}} \end{bmatrix}$$

The TRL calibration then solves the following three simultaneous equations to calculate the error matrices [4]:

$$R_{T-meas} = E_A R_{T-ideal} E_B R_{R-meas} = E_A R_{R-ideal} E_B R_{L-meas} = E_A R_{L-ideal} E_B$$

where R_{T-raw}, R_{R-raw} and R_{L-raw} can be calculated from the measured S-parameters of Thru, Reflect, and Line calibration standards, respectively. For the ideal cascade matrices $R_{T-ideal}$, as it is a zero-length Thru, achieved by connecting the VNA ports together directly, forward and reverse transmission can be considered as 1 in linear magnitude terms, and reflection can be considered as 0. For ideal $R_{R-ideal}$, we consider there to be no transmission between ports. Note that the only requirement for the TRL scheme is having a pair of identical Reflect standards with the phase known within $\pm 90^\circ$ [5]. Finally, for $R_{L-ideal}$, we consider zero reflection and transmission to be $e^{-\gamma l}$, where γ is the propagation constant, and l is the Line length. For more detailed discussion of the TRL calibration algorithm, readers can find a comprehensive explanation in [9].

2.2. TRL Line Standards

In this work, we focus on the application of the TRL calibration for coaxial connectors. Lengths of precision air-dielectric coaxial line, or airlines, are widely used as reference standards for impedance measurements in coaxial line systems [18,19]. These consist of a center and outer conductor, which, when mounted to test ports of a VNA, form an 'ideal' section of a coaxial line. With air as the dielectric, their characteristic impedance can be modeled accurately using lossy transmission line theory [20]. Precision measurements of the diameters of the center and outer conductors of the airlines using air gauging and laser gauging techniques provide metrological traceability for the use of these artifacts via the SI base unit of length, the meter. Applying them in a VNA calibration scheme such as TRL subsequently enables traceable S-parameter measurements to be made using these instruments. The specific Line standards used for this work will be discussed later in Section 2.3.

In this work, we focus on addressing a critical disadvantage of the TRL calibration compared to other schemes, such as SOLT, which is its limited frequency bandwidth. The accuracy of the TRL calibration is highly dependent on the precise determination of the transmission Line standards' phase information. A 90° phase shift provides the most distinct information from the Thru standard [21]. This maximizes the mathematical separation between the two standards, leading to more accurate calculation of the error terms.

However, when the Line standard has a 0° phase shift, it effectively behaves like the Thru standard. This causes the Thru and Line standards to become mathematically indistinguishable, making it impossible to solve all the necessary error terms. Typically, a relative phase shift of between 30° and 150° is sufficient to successfully distinguish between

the Thru and Line standards, leading to a successful TRL calibration. Therefore, the Line standard's length must comply with the following criteria:

$$\phi = 30^{\circ} \leq \frac{2\pi \cdot f \cdot l \cdot \sqrt{\varepsilon_r}}{c} \leq 150^{\circ} \quad (1)$$

where f is the frequency and ε_r is the relative permittivity of the transmission media. As a result, using a Line standard with an inappropriate length can cause multiple calibration failures throughout the desired measurement bandwidth. Figure 2a shows examples of those failure points using a single-line TRL calibration scheme. Depending on the length of the Line standard, a severe calibration failure appears in the final S-parameter results. Figure 2b shows the calculated normalized standard deviation extracted using various Line standards' extracted propagation constant (γ) from the TRL calibration algorithm using methods from [22]. At frequency points with a 90° relative phase delay, the standard deviation value is 1, representing the ideal scenario. As the phase shift approaches 0° or 180°, the normalized standard deviation value increases exponentially, indicating that the calibration accuracy is significantly degraded.

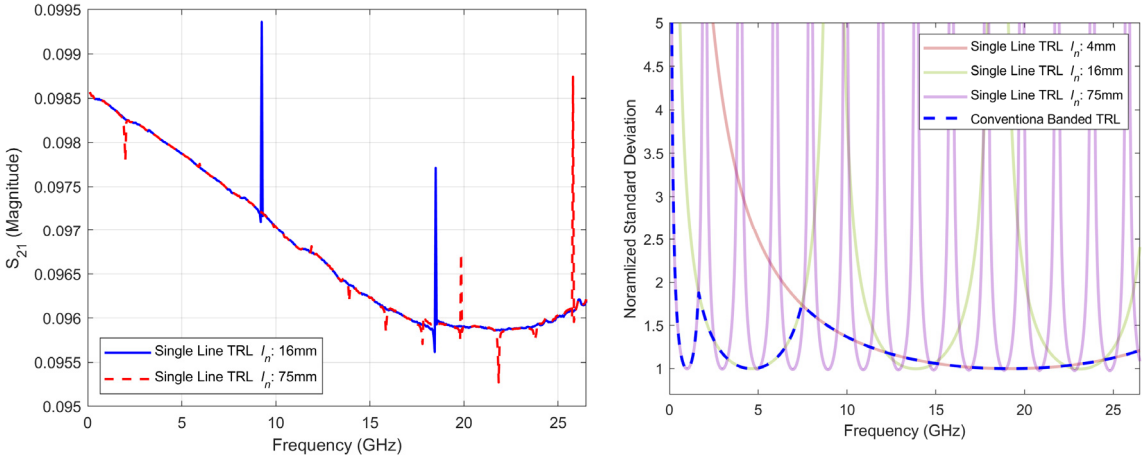

Figure 2. Examples of TRL calibration failure: (**a**) measured transmission response of a 20 dB attenuator; (**b**) normalized standard deviation of Line standards.

Due to these limitations, several Line standards with varying lengths are needed for a conventional banded-TRL scheme in order to cover a broad frequency bandwidth. As Figure 2a demonstrates, three Line standards with different lengths can exhibit multiple failure points depending on their specific length. However, by stitching the results from these three lines together, the calibration accuracy can be improved.

Figure 3 shows the workflow of the conventional banded-TRL calibration scheme that utilizes a pre-assigned frequency band for each Line standard. Firstly, conventional TRL calibration is performed for each Line standard, and the error correction is applied to the device. Following pre-assigned frequency bands, typically from manufacturer's specifications, the S-parameters are stitched together to form a final calibrated S-parameter.

For example, the entire operating frequency band of the 3.5 mm coaxial connector [23] can be covered using a typical off-the-shelf TRL calibration kit featuring Line standards of three different lengths: 4 mm, 16 mm, and 75 mm. These cover high-, mid-, and low-frequency ranges, respectively. Figure 4a,b show an example of the same DUT calibrated with the 'Banded-TRL' method. By using this method, the TRL failures shown in Figure 2a are no longer visible.

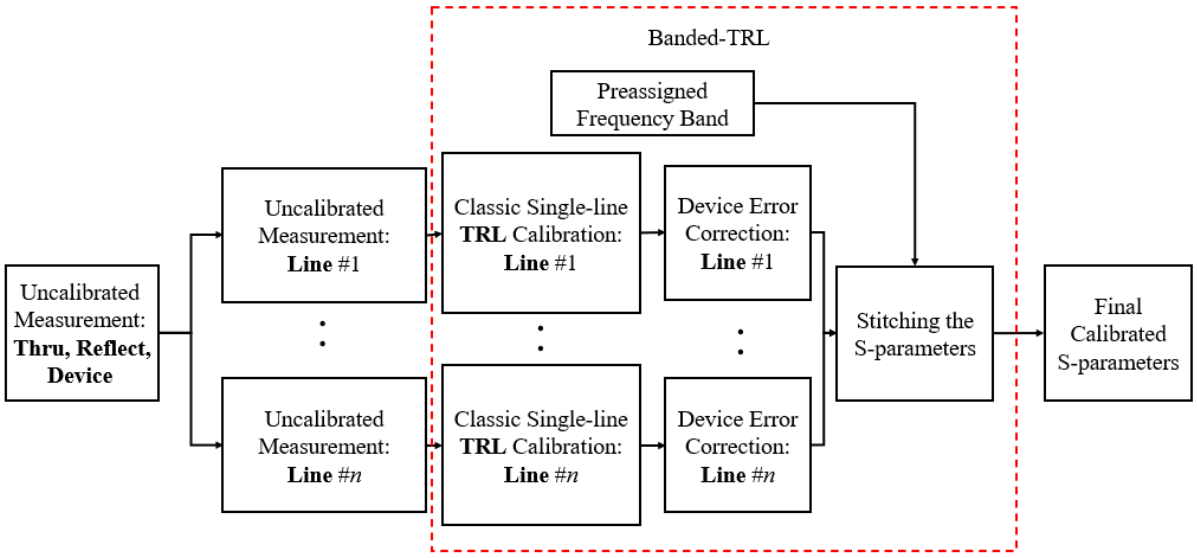

Figure 3. Workflow of the conventional banded-TRL calibration scheme.

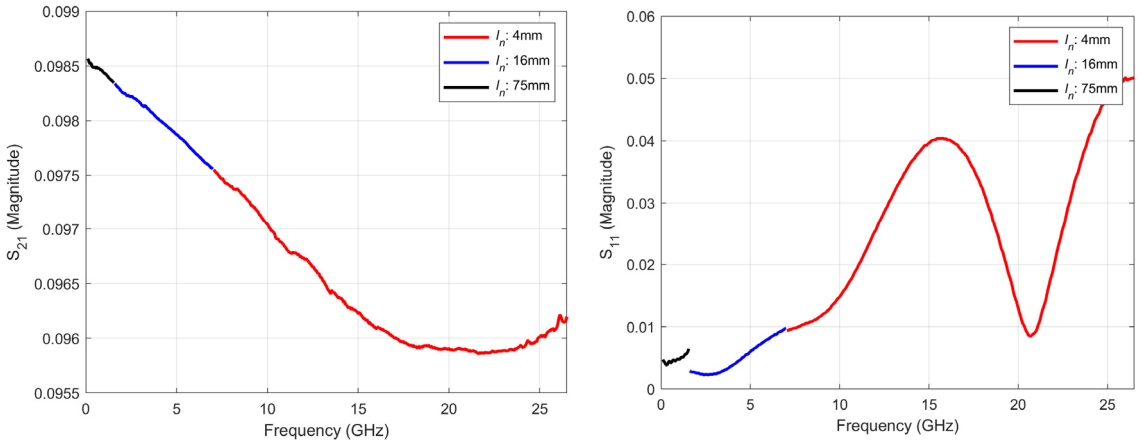

Figure 4. Banded-TRL (Line standard lengths (l_n): 4 mm, 16 mm, 75 mm) calibrated S-parameters of 3.5 mm 20 dB attenuator: (**a**) transmission response; (**b**) reflection response.

However, the banded-TRL method has another issue. From Figure 4b, noticeable step changes can be observed in the S_{11} response at the frequencies where the calibration shifts from one Line standard to the next. This is due to the slight differences in impedance between each Line standard [11]. In this example, precision air-dielectric coaxial calibration standards are used. These Line standards are widely used for primary-level calibration as their characteristic impedances (Z_0) are dependent on the Line standards' center and outer conductor dimensions, as shown in this simplified equation [24]:

$$Z_0 = \frac{\sqrt{\mu\varepsilon}}{2\pi}\ln\left(\frac{b}{a}\right) \tag{2}$$

where μ is free space permeability, ε is the permittivity, and a and b are the radii of the center and outer conductors. Due to manufacturing tolerances, the dimensions will not always be perfect; hence, the impedance between standards will vary. Furthermore, the connection of the airline to the VNA test ports is a challenging task, and, thus, use of airlines will suffer from connection non-repeatability [25]. It is these factors that contribute to the step changes in the results.

To address these discontinuities, various weighting schemes can be introduced [16]. Our proposed weighting scheme directly addresses these phase-related issues. By automatically assigning a greater weight to Line standards with relative phase shifts closer to 90°, we mitigate the detrimental effects of phase errors. Figure 5 shows the workflow of the weighted-TRL calibration scheme presented in this work. Firstly, as with the banded-TRL calibration, conventional single-line TRL calibration is performed for each Line standard, and the error correction is applied to the DUT measurements. Using the phase information extracted from the TRL calibration algorithm, the weights are assigned for each Line standard. Results are combined using the weighting function to give the final calibrated DUT S-parameters. In our demonstrations, we use three and six different Line standards for 3.5 mm and Type-N calibrations, respectively.

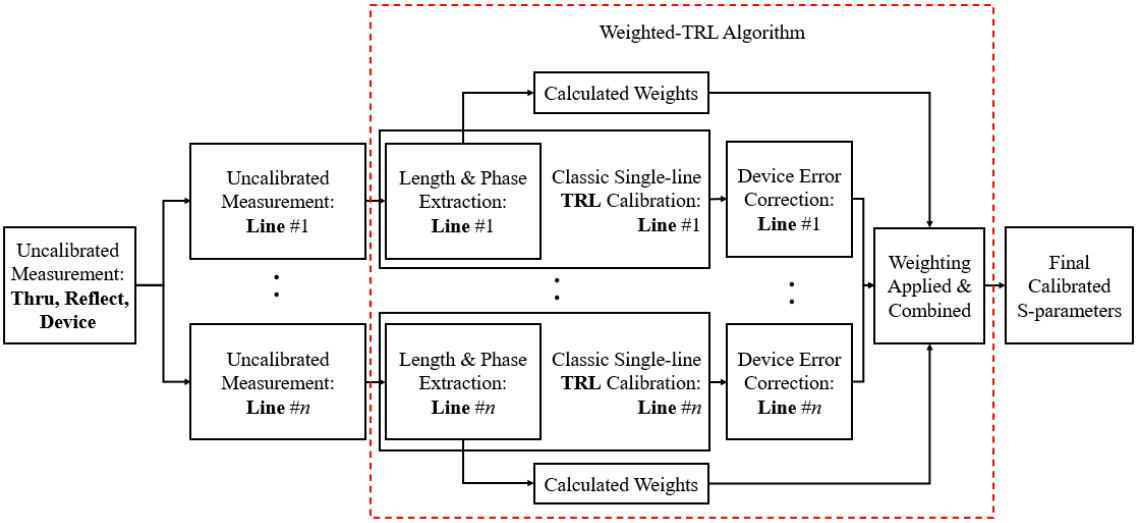

Figure 5. Workflow of the weighted-TRL calibration scheme proposed in this work.

2.2.1. Weighting Equation

Here are the most important criteria for selecting a weighting equation to be used for the TRL calibration results. At the frequency points where the relative phase (ϕ_i) of the selected i_{th} line is 90°, i.e., where the confidence of the calibration is the highest, a maximum weighting value of $w_i = 1$ is assigned by the scheme. For the frequency points where $\phi_i = 180°$, i.e., where the confidence of the TRL calibration is at the lowest level, the weighting value $w_i = 0$ is assigned. The transition has to be smooth for the frequency points between these two points to avoid the discontinuities mentioned above. In this study, two different equations were utilized. Firstly, weights are determined using a function (T_{2n}) following:

$$T_{2n}(\phi_i) = w_i = \sin^{2n}\phi_i \tag{3}$$

where n is an integer coefficient that can be used to vary the shape of the function. It is important to note that as the weights cannot be negative integers, for Equation (3), power coefficients need to be even integers. Therefore, the integer coefficient n is multiplied by 2, another function that meets the criterion uses the following equation.

$$G_n(\phi_i) = w_i = -\frac{1}{2}\cdot\sqrt{\frac{1+n^2}{(1+n^2\cos(2\phi_i))^2}}\cdot\cos(2\phi_i) + 1 \tag{4}$$

Calculated weights using the two functions with varying integer coefficients are shown in Figure 6. Note that Figure 6 only displays relative phase values between 0 and $\pi/2$, as the behavior for values between $\pi/2$ and π is symmetrical.

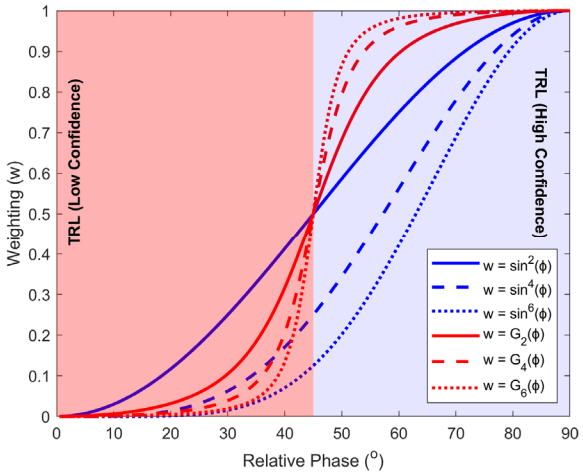

Figure 6. TRL weighting function comparison.

Figure 6 illustrates that all the functions adhere to the established criteria. With the T_{2n} function, increasing n enhances rejection characteristics at low confidence levels but narrows at high confidence coverage. Conversely, increasing n in the G_n function improves coverage at both high and low confidence, albeit with a steeper transition. This suggests that simply increasing the coefficient may not inherently optimize the TRL calibration.

Table 1 details the areas under each curve for the acceptable and failure TRL regions. For the T_{2n} function, $n = 2$ is selected due to its favorable balance of TRL failure rejection and acceptable area coverage, maintaining at least 50% coverage. In the case of the G_n function, $n = 4$ is chosen since increasing the coefficient beyond this point yields diminishing returns in TRL acceptable area coverage while also steepening the transition. It is important to note that while our current parameter choices appear optimal for the scenarios explored in this work, further investigation involving a larger and more diverse set of calibration runs and DUTs is necessary to definitively establish their universal optimality. A comprehensive sensitivity analysis, examining the impact of parameter variations on calibration performance across a broader range of scenarios, will feature in future work.

Table 1. Area coverage of each function.

	TRL Failure Area Coverage ($0^\circ < \phi_i < 30^\circ$)		**TRL Acceptable Area Coverage** ($30^\circ < \phi_i < 90^\circ$)	
	T_{2n}	G_n	T_{2n}	G_n
$n = 1$	8.7%	5.5%	71%	72%
$n = 2$	1.3%	2.7%	56%	74%
$n = 3$	0.2%	1.5%	47%	74%
$n = 4$	0.05%	0.9%	41%	75%
$n = 5$	0.01%	0.6%	37%	75%
$n = 6$	0.02%	0.4%	34%	75%

After calculating the weights for each frequency, the final S-parameter (S_f) is determined applying the weighted mean Equation (5) to the S-parameter calibrated with each Line standard (S_i).

$$S_f = \frac{\sum_{i=1}^{3} w_i S_i}{\sum_{i=1}^{3} w_i} \tag{5}$$

2.2.2. Length and Phase Determination

As discussed in the previous subsection, the phase of each Line standard needs to be determined first to subsequently determine the weights. The easiest way of determining the relative phase is by measuring the physical length of the transmission line and converting it

to the relative phase using Equation (1). However, for some cases, where mechanical length measurement is not applicable (i.e., non-air dielectric), the estimated length can be extracted during the TRL calibration process following the process described in [9]. Assuming the Line standards are perfectly matched and do not have any significant reflection, the cascade matrices for the measured Line standard and zero-length Thru are:

$$R_{L-meas} = E_A \begin{pmatrix} e^{-\gamma l_i} & 0 \\ 0 & e^{\gamma l_i} \end{pmatrix} E_B \; ; \; R_{T-Meas} = E_A \begin{pmatrix} 1 & 0 \\ 0 & 1 \end{pmatrix} E_B \tag{6}$$

By combining the Line and Thru standard matrices, the following relationship can be found:

$$R_{L-meas}\, R_{T-meas}^{-1} E_A = E_A \begin{pmatrix} e^{-(\alpha+j\beta)l_i} & 0 \\ 0 & e^{(\alpha+j\beta)l_i} \end{pmatrix} \tag{7}$$

where α is the attenuation constant and β is the phase constant. In solving this equation, the term $e^{2(\alpha+j\beta)l_i}$ can be extracted. The detailed process can be found in [9,26]. Finally, using the complex part (phase constant β) of the term, Line length information can be extracted from the result at each frequency point.

2.3. Precision Airline Calibration Standard

Precision coaxial airline calibration standards in two coaxial connector sizes were used to verify the proposed weighted-TRL calibration schemes. First, three airline standards from an off-the-shelf TRL calibration kit for the 3.5 mm connector were used. These have nominal lengths of 75 mm, 16 mm, and 4 mm. Next, six airline standards in the Type-N connector were used with nominal lengths of 150 mm, 125 mm, 49 mm, 42 mm, 38 mm, and 31 mm. The 16 mm and 31 mm airlines in the 3.5 mm and Type-N connector sizes are shown in Figure 7a,b, respectively.

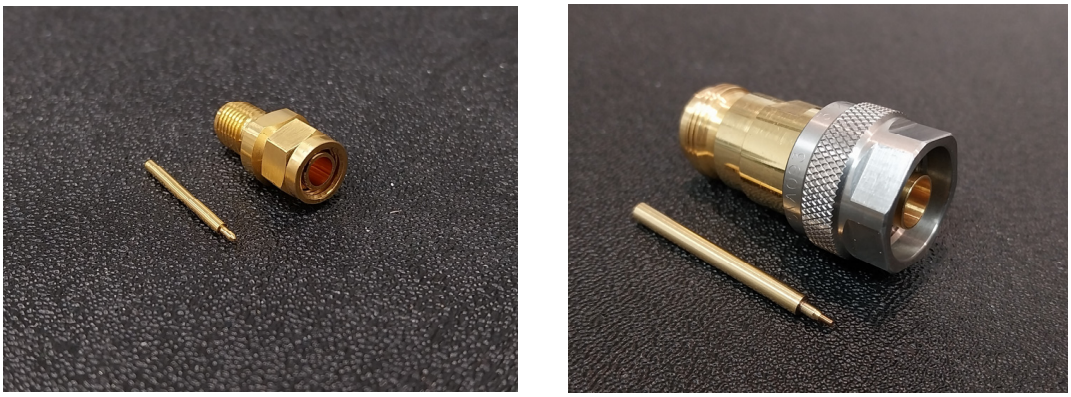

(**a**) (**b**)

Figure 7. Precision airline standards: (**a**) 3.5 mm; (**b**) Type-N.

3. Results

3.1. Length Extraction

Figure 8a,b show the extracted length (l_{ext}) distribution for the 3.5 mm and Type-N Line standards. Using the mode or median of the distributed length, the relative phase of each Line standard is determined using Equation (1). Note that as the Line standards used in this case have air as the dielectric, the mechanical lengths (either measured or nominal lengths given by manufacturer) can also be used. The length values indicated in Figure 8 are used to calculate the corresponding weights. Figure 8 also shows the nominal lengths (l_{nom}) of the Line standards.

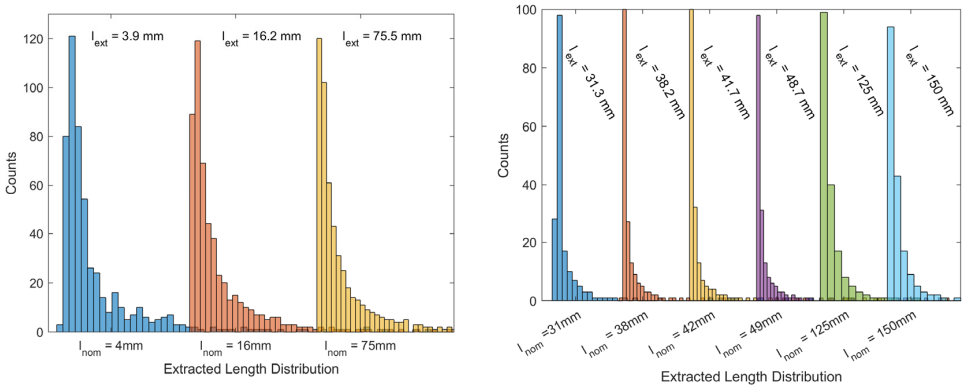

Figure 8. Histogram chart showing TRL calculated length distribution: (**a**) 3.5 mm Line standards; (**b**) Type-N Line standards.

3.2. 3.5 mm Results

Figure 9a,b show the S-parameter results of a 20 dB attenuator, both measured and calibrated using the weighted-TRL methods described earlier. A significant improvement can be seen from the figures, as the discontinuity due to the step changes associated with banded-TRL calibration is absent. This indicates that both of the weighting functions are very effective for smoothing the frequency transitions between different Line standards. In addition, there is no noticeable difference between the results obtained using the two weighting functions (T_4 and G_4). This suggests that both functions are equally effective for consistent calibration results.

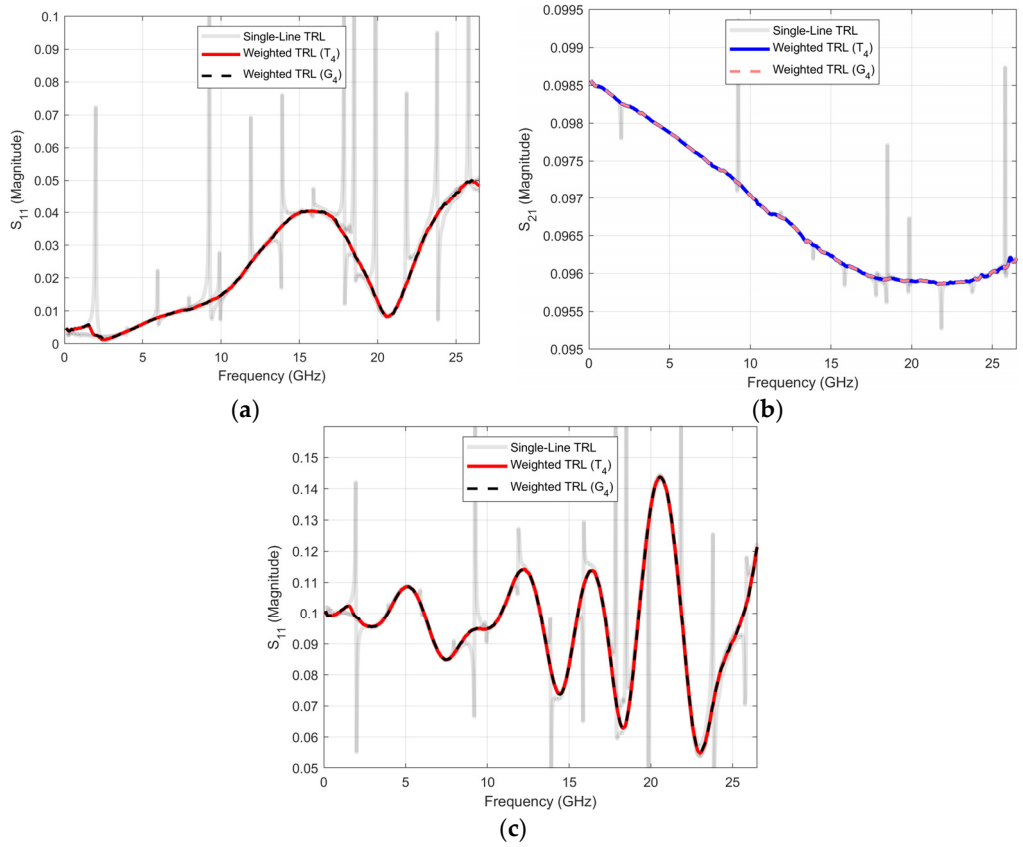

Figure 9. Weighted-TRL (Line lengths (l_n): 4 mm, 16 mm, 75 mm) calibrated S-parameters of 3.5 mm devices: (**a**) 20 dB attenuator (S_{11}); (**b**) 20 dB attenuator (S_{21}); (**c**) short with 10 dB attenuator (S_{11}).

Figure 9c shows the S-parameter results for a 10 dB attenuator terminated with a short circuit. Like the previous case, the step-change discontinuities are eliminated, demonstrating the versatility of the weighted-TRL method in handling different device responses. In both scenarios, the two weighting functions successfully remove calibration failures and discontinuities. This reinforces the conclusion that the weighted-TRL calibration technique offers a robust solution for a broad range of frequencies and various device types.

3.3. Type-N Results

Figure 10 shows the measured and calibrated S-parameter results of a 20 dB attenuator with Type-N connectors. Consistent with the previous 3.5 mm results, applying the weighted-TRL calibration eliminates the step changes previously evident in the unweighted, banded-TRL calibration. This further validates the efficacy of the weighting functions in mitigating discontinuities and TRL calibration failures. Also, as observed in the 3.5 mm device measurements, both weighting functions (T_4 and G_4) show identical results, indicating their robustness and interchangeability in achieving a good VNA calibration.

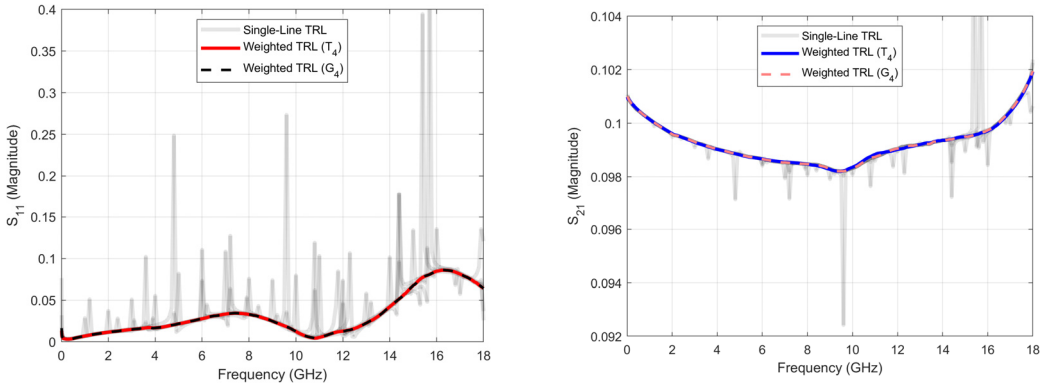

Figure 10. Weighted-TRL (airline-line standard lengths (l_n): 4 mm, 16mm, 75 mm) calibrated S-parameters of Type-N devices: (**a**) 20 dB attenuator (S_{11}); (**b**) 20 dB attenuator (S_{21}).

Notably, the weighted-TRL calibration scheme offers an additional advantage over the banded-TRL approach. Utilizing every Line standard across the entire frequency band introduces an averaging effect that effectively mitigates the impact of random errors such as connection repeatability.

4. Limitations

While the weighted-TRL calibration method proposed in this work effectively addresses the issue of step changes and improves the overall accuracy of TRL calibration, it is important to recognize its limitations. The method cannot eliminate all potential error sources in the VNA calibration and measurement processes. Factors such as connector repeatability, where variations in connection quality can lead to inconsistent measurements, remain challenges. Cable stability can also cause significant impacts, as changes in cable properties due to excessive and uneven bends, changes in temperature, or aging can cause measurement errors and drift errors. Even with careful calibration, residual errors persist due to imperfections in the calibration standards and the measurement system itself. Moreover, the DUT itself can introduce errors through parasitics, non-linearities, or sensitivity to environmental factors, which cannot be fully addressed by the proposed calibration scheme. It is crucial to consider these limitations when interpreting the results obtained using the proposed method. While it significantly improves calibration accuracy, end users must remain aware of other potential error sources and take appropriate measures to mitigate their impact. The latest in metrological guidance on addressing and accounting for these errors can be found in the EURAMET VNA guide [10].

5. Discussion and Conclusions

The results presented in this work show the effectiveness of the weighted-TRL calibration method in addressing the limitations of traditional TRL and banded-TRL approaches. Compared to traditional banded-TRL calibration, our weighted TRL algorithm not only eliminates step changes caused by impedance mismatches but also streamlines the calibration process by eliminating the need for extra dimensional measurements of the Line standards and automating phase assignment. Additionally, the built-in weighting function provides added averaging effects across the band, further enhancing calibration accuracy.

Based on Equations (3) and (4), the two weighting functions investigated demonstrate comparable performance in eliminating discontinuities and calibration failures. This suggests that the choice between these weighting functions may not be critical if it adheres to the key criteria of assigning a maximum weight at 90° relative phase and a minimum weight at 0° or 180° relative phase, with smooth transitions in between.

The successful application of this technique to measurements of both 3.5 mm and Type-N coaxial devices demonstrates its versatility and applicability to a wide range of measurement scenarios. This is particularly relevant for metrology-grade measurements, where high accuracy and reliability are essential.

It is worth noting that while the weighted-TRL method effectively addresses the issue of step changes, it does not eliminate all potential sources of error in VNA measurements. Factors such as connector repeatability, cable stability, and ambient temperature variations, among others, can still contribute to measurement uncertainties. However, by mitigating one of the major limitations of the TRL calibration, this technique represents a significant step forward in improving the overall accuracy and reliability of VNA measurements. Furthermore, in contrast with other TRL schemes [18], this weighting algorithm treats the results from each Line standard independently. This can facilitate further post-processing with respect to the differences in each specific Line, for example, impedance renormalization [27].

The method presented in this work has the potential to bring substantial improvements to VNA measurements, both for primary-level traceability [28] and in more applied scenarios. While this work focuses on typical coaxial airline-based calibration scenarios, the proposed weighted-TRL method has the potential for broader applications. For example, in cryogenic environments, where traditional TRL calibration can be affected by temperature-induced variations in components and standards, our method's robustness to phase ambiguities and impedance mismatches could lead to significantly improved accuracy. Similarly, in mm-wave and THz measurements, where connector misalignment and transmission losses become more pronounced, the weighted-TRL method's ability to leverage phase information could enable more precise calibrations.

Factors such as the frequency range, connector size, and complexity of the measurement scenario need to be considered. For example, for on-wafer measurements, customized calibration standards depending on the substrate material and probe configurations in use may be required. Additionally, for mm-wave and THz measurements, the relatively low availability of precision-machined waveguide-based calibration standards of suitable dimensions might be a limiting factor. Nevertheless, we believe that with careful consideration of these factors and potential adaptations to the calibration procedure, this weighted-TRL method can be successfully extended to a wide range of devices and measurement scenarios.

In conclusion, through the utilization of applied mathematics, this work introduces an effective solution for VNA calibration, addressing common RF-electronics measurement challenges. The proposed weighting algorithm, derived from the analysis of phase information, underscores the potential of innovative mathematical approaches to enhance measurement procedures across various domains, improving both the accuracy and robustness of results. The increased confidence in measurements this provides has the potential to provide benefits to VNA end users across numerous industrial and scientific spheres.

Future work could explore the development of more advanced weighting functions, the extension of the method to other transmission media such as waveguide and on-

wafer measurements, and its application in emerging fields such as cryogenic quantum technologies. These avenues offer exciting opportunities to further enhance the capabilities of VNA calibration and enable more precise and reliable measurements across a wide range of applications. In addition, a comprehensive calibration comparison, encompassing comparisons between the results produced by the proposed method and primary-level calibration schemes other than TRL (e.g., multiple offset-short [29]), will yield valuable insights into VNA calibration and measurement error sources and help develop strategies to mitigate them.

Author Contributions: Conceptualization, S.-h.S.; methodology, S.-h.S. and J.S.; validation, S.-h.S. and J.S.; investigation, S.-h.S. and J.S.; data curation, J.S.; writing—original draft preparation, S.-h.S.; writing—review and editing, S.-h.S. and J.S. All authors have read and agreed to the published version of the manuscript.

Funding: This work was supported by the IITP (Institute of Information & Communications Technology Planning & Evaluation)-ITRC (Information Technology Research Center) grant funded by the Korean government (Ministry of Science and ICT) (IITP-2024-RS-2024-00437191). This work was also supported by the faculty research fund of Sejong University in 2024.

Data Availability Statement: The raw data supporting the conclusions of this article will be made available by the authors on request.

Conflicts of Interest: The authors declare no conflicts of interest.

References

1. Stanley, M.; Shang, X.; Celep, M.; Salter, M.; de Graaf, S.; Lindstrom, T.; Shin, S.-H.; Skinner, J.; Singh, S.; Stokes, S.; et al. RF and microwave metrology for quantum computing—Recent developments at the UK's National Physical Laboratory. *Int. J. Microw. Wirel. Technol.* **2024**, 1–9. [CrossRef]
2. Horibe, M.; Kato, Y.; Sakamaki, R. Electromagnetic Measurement Techniques for Materials and Device Used in 6G Wireless Communications. In Proceedings of the 2020 2nd 6G Wireless Summit (6G SUMMIT), Levi, Finland, 18–19 March 2020; pp. 1–5.
3. Stănculescu, M.; Iordache, L.; Iordache, M.; Niculae, D.; Bucată, V. Using S parameters in wireless power transfer analysis. In Proceedings of the 2017 10th International Symposium on Advanced Topics in Electrical Engineering (ATEE), Bucharest, Romania, 23–25 March 2017; pp. 107–112.
4. Estrada, A. The vector network analyzer—An essential tool in modern ATE measurements. *IEEE Instrum. Meas. Mag.* **2012**, *15*, 22–26. [CrossRef]
5. Rumiantsev, A.; Ridler, N. VNA calibration. *IEEE Microw. Mag.* **2008**, *9*, 86–99. [CrossRef]
6. Rytting, D. Advances in microwave error correction techniques. In Proceedings of the Hewlett-Packard RF and Microwave Measurement Symposium and Exhibition, Santa Clara, CA, USA, 10–11 June 1987; pp. 6201–6302.
7. Fitzpatrick, J. Error models for systems measurement. *Microw. J.* **1978**, *21*, 63–66.
8. Eul, H.-J.; Schiek, B. A generalized theory and new calibration procedures for network analyzer self-calibration. *IEEE Trans. Microw. Theory Tech.* **1991**, *39*, 724–731. [CrossRef]
9. Engen, G.F.; Hoer, C.A. Thru-reflect-line: An improved technique for calibrating the dual six-port automatic network analyzer. *IEEE Trans. Microw. Theory Tech.* **1979**, *27*, 987–993. [CrossRef]
10. EA. *Guidelines on the Evaluation of Vector Network Analysers (VNA): Calibration Guide No. 12, version 3.0*; EURAMET: Braunschweig, Germany, 2018.
11. Stokes, D.; Gellersen, F.; Allal, D.; Skinner, J.; Phung, G.N.; Kuhlmann, K. Traceable S-parameter measurements up to 90 GHz in 1.35 mm coaxial. *Meas. Sci. Technol.* **2023**, *34*, 064006. [CrossRef]
12. Koo, H.; Cho, C.; Kang, T.-W.; Kwon, J.Y. Pin-Gap Correction of Coaxial Calibration Standards for TRL or LRL Calibration. *IEEE Access* **2022**, *10*, 34779–34788. [CrossRef]
13. Gellersen, F.; Kuhlmann, K.; Rausche, F. VNA Calibration using Coaxial Air Lines with Two Plug Connectors. In Proceedings of the 2023 53rd European Microwave Conference (EuMC), Berlin, Germany, 19–21 September 2023; pp. 608–611. [CrossRef]
14. Jargon, J.A.; Williams, D.F.; Long, C.J.; Hagerstrom, A.M.; Stelson, A.C.; Ren, W. *Physical Models and Dimensional Traceability of 2.4 mm Coaxial Airline Standards for Determining Systematic Uncertainties of Calibrated Scattering-Parameters*; NIST Technical Note TN225; US Department of Commerce, National Institute of Standards and Technology: Gaithersburg, MD, USA, 2023.
15. Ridler, N.M.; Clarke, R.G.; Li, C.; Salter, M.J. Strategies for traceable submillimeter-wave vector network analyzer measurements. *IEEE Trans. Terahertz Sci. Technol.* **2019**, *9*, 392–398. [CrossRef]
16. Shin, S.-H.; Stanley, M.; Skinner, J.; de Graaf, S.E.; Ridler, N.M. Broadband Coaxial S-Parameter Measurements for Cryogenic Quantum Technologies. *IEEE Trans. Microw. Theory Tech.* **2024**, *72*, 2193–2201. [CrossRef]

17. Stanley, M.; Shin, S.-H.; Skinner, J.; Urbonas, J.; Ridler, N. Characterising Scattering Parameters of Coaxial Microwave Devices at Milli-kelvin Temperatures for Quantum Computing Technologies. In Proceedings of the 2023 53rd European Microwave Conference (EuMC), Berlin, Germany, 19–21 September 2023; pp. 150–153.
18. Eiø, C.P.; Protheroe, S.J.; Ridler, N.M. Characterising beadless air lines as reference artefacts for S-parameter measurements at R.F. and microwave frequencies. *Proc. Inst. Elect. Eng. Sci. Meas. Technol.* **2006**, *153*, 229–234. [CrossRef]
19. Harris, I.A.; Spinney, R.E. The realization of high-frequency impedance standards using air-spaced coaxial lines. *IEEE Trans. Instrum. Meas.* **1964**, *13*, 265–272. [CrossRef]
20. Daywitt, W.C. First-order symmetric modes for a slightly lossy coaxial transmission line. *IEEE Trans. Microw. Theory Tech.* **1990**, *38*, 1644–1651. [CrossRef]
21. Hoer, C.A. Choosing line lengths for calibrating network analyzers. *IEEE Trans. Microw. Theory Tech.* **1983**, *31*, 76–78. [CrossRef]
22. Marks, R.B. A Multiline Method of Network Analyzer Calibration. *IEEE Trans. Microw. Theory Tech.* **1991**, *39*, 1205–1215. [CrossRef]
23. *IEEE Std 287.1-2021*; IEEE Standard for Precision Coaxial Connectors at RF, Microwave, and Millimeter-Wave Frequencies—Part 1: General Requirements, Definitions, and Detailed Specifications. IEEE: Piscataway, NJ, USA, 2022; pp. 1–136.
24. Juroshek, J.R.; Free, G.M. Measurements of the characteristic impedance of coaxial air line standards. *IEEE Trans. Microw. Theory Tech.* **1994**, *42*, 186–191. [CrossRef]
25. Mubarak, F.; Hoffmann, J. Effects of connectors and improper mounting of air lines in TRL calibration. In Proceedings of the 2016 Conference on Precision Electromagnetic Measurements (CPEM 2016), Ottawa, ON, Canada, 10–15 July 2016; pp. 1–2.
26. Schumann, U.; Jöstingmeier, A.; Omar, A. Analytical Considerations of the TRL Calibration Procedure for General De-Embedding Purposes. In Proceedings of the 2019 42nd International Spring Seminar on Electronics Technology (ISSE), Wroclaw, Poland, 14–17 May 2019; pp. 1–4.
27. Kuhlmann, K. A study of the reference impedance influence on a TRL calibration. In Proceedings of the 2016 87th ARFTG Microwave Measurement Conference (ARFTG), San Francisco, CA, USA; 2016; pp. 1–4.
28. Mubarak, F.A.; Rietveld, G. Uncertainty evaluation of calibrated vector network analyzers. *IEEE Trans. Microw. Theory Tech.* **2018**, *66*, 1108–1120. [CrossRef]
29. Horibe, M.; Kishikawa, R. Precision Offset Short Calibration Standards for 1.35 mm Coaxial Line Sizes. In Proceedings of the 2021 97th ARFTG Microwave Measurement Conference (ARFTG), Atlanta, GA, USA; 2021; pp. 1–4. [CrossRef]